International Journal for Parasitology 52 (2022) 581–590

Contents lists available at ScienceDirect

International Journal for Parasitology

journal homepage: www.elsevier.com/locate/ijpara

Ubiquitination pathway model for the barber's pole worm – *Haemonchus contortus*

Yuanting Zheng [a], Guangxu Ma [a,b], Tao Wang [a], Andreas Hofmann [a,c], Jiangning Song [d,e,f], Robin B. Gasser [a,*], Neil D. Young [a,*]

[a] Department of Veterinary Biosciences, Melbourne Veterinary School, The University of Melbourne, Parkville, Victoria, Australia
[b] College of Animal Sciences, Zhejiang Provincial Key Laboratory of Preventive Veterinary Medicine, Zhejiang University, Hangzhou, China
[c] Max Rubner-Institut, Federal Research Institute of Nutrition and Food, Kulmbach, Germany
[d] Department of Data Science and AI, Faculty of IT, Monash University, Victoria, Australia
[e] Biomedicine Discovery Institute and Department of Biochemistry and Molecular Biology, Monash University, Victoria, Australia
[f] Monash Data Futures Institute, Monash University, Victoria, Australia

ARTICLE INFO

Article history:
Received 22 March 2022
Received in revised form 10 June 2022
Accepted 11 June 2022
Available online 16 July 2022

Keywords:
Ubiquitination pathway
Haemonchus contortus
Parasitic worm
Informatics
Transcription

ABSTRACT

The ubiquitin-mediated pathway has been comprehensively explored in the free-living nematode *Caenorhabditis elegans*, but very little is known about this pathway in parasitic nematodes. Here, we inferred the ubiquitination pathway for an economically significant and pathogenic nematode – *Haemonchus contortus* – using abundant resources available for *C. elegans*. We identified 215 genes encoding ubiquitin (Ub; n = 3 genes), ubiquitin-activating enzyme (E1; one), -conjugating enzymes (E2s; 21), ligases (E3s; 157) and deubiquitinating enzymes (DUBs; 33). With reference to *C. elegans*, Ub, E1 and E2 were relatively conserved in sequence and structure, and E3s and DUBs were divergent, likely reflecting functional and biological uniqueness in *H. contortus*. Most genes encoding ubiquitination pathway components exhibit high transcription in the egg compared with other stages, indicating marked protein homeostasis in this early developmental stage. The ubiquitination pathway model constructed for *H. contortus* provides a foundation to explore the ubiquitin–proteasome system, crosstalk between autophagy and the proteasome system, and the parasite-host interactions. Selected E3 and DUB proteins which are very divergent in sequence and structure from host homologues or entirely unique to *H. contortus* and related parasitic nematodes may represent possible anthelmintic targets.

1. Introduction

Protein turnover is a crucial mechanism in cells ensuring a healthy state, with misfolded and damaged proteins needing to be eliminated to maintain physiological cellular metabolism (Goldberg, 2003). The major protein degradation pathway in eukaryotic cells operates via the ubiquitin–proteasome system (UPS), which also associates with processes including inflammation, cell differentiation, cell proliferation and DNA repair (Wang and Maldonado, 2006; Daulny and Tansey, 2009). The process of protein degradation through UPS is composed of two main elements: (i) the ubiquitination pathway and (ii) the proteasome complex (Glickman and Ciechanover, 2002). In UPS, the ubiquitination pathway plays a central role in determining the fate of a substrate protein – sometimes referred to as "the kiss of death" (Behuliak et al., 2005). The ubiquitination system of eukaryotes comprises a series of components, including ubiquitin (Ub), the ubiquitin-activating enzyme (E1), ubiquitin-conjugating enzyme (E2), ubiquitin ligase (E3) and deubiquitinating enzyme (DUB) (Pickart and Eddins, 2004). The ubiquitination process is triggered by E1, which activates Ub through the formation of a thioester bond between the C-terminus of Ub and the corresponding cysteine of E1 (Haas et al., 1982). After Ub is activated, it is transferred to E2 via a thioester bond formation from E1 to a cysteine residue of E2 (Liu et al., 2020). Then, a substrate-specific E3 facilitates the transfer of the Ub from E2 to a target substrate (Komander and Rape, 2012). These steps are repeated several times to produce poly-Ub chains on a protein substrate (Nguyen et al., 2014). Ubiquitin is usually a 76-amino acid protein that has seven lysine residues, all of which are potential conjugation sites; however, only the poly-Ub chains conjugated on the Lys-48 can be recognised and degraded via the UPS (Hershko and Ciechanover, 1998). The

* Corresponding authors.
E-mail addresses: robinbg@unimelb.edu.au (R.B. Gasser), nyoung@unimelb.edu.au (N.D. Young).

https://doi.org/10.1016/j.ijpara.2022.06.001
0020-7519/

number of Ub monomers within a poly-Ub chain determines the fate of conjugated substrates: the targeted substrate is processed by the UPS only if there are more than four Ub monomers in the chain; otherwise, they are modified to take part in other proteasome-independent cellular processes such as transcriptional regulation, cell differentiation and signal transduction (Kallio et al., 1999; Guo et al., 2004). E1 has an NAD-binding domain (Pickart and Eddins, 2004). E2 contains one domain (called UBC) of 150 amino acids which is recognised by E3 (VanDemark and Hill, 2002). In contrast, many distinct E3 components are known, namely HECT domain protein, U-box domain protein, monomeric really interesting new gene (RING) finger domain protein, multi-subunit RING finger complex (cullin-based) and multi-subunit RING finger complex (APC/C-based) (Kipreos, 2005). The formation of Ub chains is a reversible process, and DUB cleaves Ub from substrates and Ub-chains (Reyes-Turcu et al., 2009).

The ubiquitination pathway has been extensively studied in the free-living nematode *Caenorhabditis elegans* (see Kipreos, 2005; Papaevgeniou and Chondrogianni, 2014) – one of the best characterised metazoan organisms (Nigon and Félix, 2017). However, nothing is known about this pathway in most parasitic worms. Clearly, the wealth of molecular data sets and information on *C. elegans* provide a unique opportunity to commence exploring the ubiquitination pathway system in related parasitic nematodes for which high-quality genomes and transcriptomes exist. *Haemonchus contortus* – the barber's pole worm – is one such nematode; it is a highly significant pathogen of ruminants (Gasser and von Samson-Himmelstjerna, 2016). This species and its relatives (members of the superfamily Trichostrongyloidea) have become challenging to control in livestock animals due to widespread resistances in worms to currently used anthelmintics. The extensive genomic, transcriptomic, proteomic and lipidomic resources now available for *H. contortus* (see Laing et al., 2013; Schwarz et al., 2013; Gasser et al., 2016; Doyle et al., 2018, 2020; Ma et al., 2018, 2020; Wang et al., 2019a,b, 2020a,b) should enable the pursuit of alternative approaches of treatment or control, building on a sound understanding of key molecular or biochemical processes or pathways, such as ubiquitination (Kipreos, 2005). In particular, the ubiquitination pathway is known to contain druggable targets (e.g., E1, E2 and E3) for treatments of cancers (Zhang et al., 2020) and schizophrenia (Luza et al., 2020). As a first step toward exploring the potential of molecular components in this pathway as potential anthelmintic targets, we constructed here a model of the ubiquitination pathway of *H. contortus*.

2. Materials and methods

2.1. Identification of C. elegans gene homologues in H. contortus

Gene and protein sequence data representing Ub and E1, E2, E3 and the DUB enzymes of *C. elegans* were retrieved from WormBase (version WS278; https://wormbase.org) and associated information from published literature (Jones et al., 2002; Kipreos, 2005; Papaevgeniou and Chondrogianni, 2014; Supplementary Table S1). Genomic (from ISE/inbred ISE strains) and transcriptomic (from the Haecon-5 strain) data sets for *H. contortus* were obtained from WormBase-ParaSite (version WBPS15; https://parasite.wormbase.org/; Howe et al., 2017).

Homologues of *C. elegans* genes in the *H. contortus* genome were initially identified using the BlastP algorithm (Johnson et al., 2008) using an E-value cut-off value of $<10^{-5}$. The sequences representing individual gene families/groups in *C. elegans* were aligned to build a Hidden Markov Model (HMM) model. The pre-calculated HMM models for ubiquitin (Pfam database accession PF00240), UBA_e1_thiolCys (PF10585), UQ_con (PF00179), HECT (PF00632), U-box (PF04564), RING (CL0229), cullin (PF00888), F-box (PF00646), VHL (PF01847), BTB (PF00651), OTU (PF02338), JAB (PF01398), UCH (PF00443) and peptidase_C12 (PF01088) were downloaded from Pfam (https://pfam.xfam.org/) and used to verify the outcome of the homology search and support homology-inferred annotation. HMMER3 (https://hmmer.org/) was used to search for matching homologues (complete sequences) in *H. contortus* with a threshold of E-value cut-off of <0.01 (Eddy, 2009). Subsequently, LAST (Kiełbasa et al., 2011) was used to distinguish ubiquitin from ubiquitin-like proteins by directly aligning their sequences. Clustal W (Larkin et al., 2007) was used to align the UBC domain of inferred proteins to verify the presence of a catalytic core. Sequences without an active-site cysteine residue were classified into a separate group of proteins (designated 'ubiquitin E2 variants', UEVs), according to a previous study (Jones et al., 2002). Reciprocal BlastP comparisons were conducted to identify and verify the identity of orthologues, and RNA-seq data were used to assess transcription and to curate the gene models (cf. Stroehlein et al., 2018; Ma et al., 2019). Following the identification of orthologous genes in *H. contortus*, protein sequences were inferred and then mapped to the predicted proteome of *Ovis aries* (sheep) (Archibald et al., 2010) using the BlastP program (Johnson et al., 2008) to identify host orthologues. Again, reciprocal BlastP comparisons was performed to verify orthology.

2.2. Analyses of sequence features and chromosomal localisation

The molecular weight (MW) and isoelectric point (pI) of protein sequences encoded by the genes identified were estimated using online tools available via ExPASy (https://www.expasy.org/; Gasteiger et al., 2003). Conserved domains in proteins were inferred using CD-Search (Marchler-Bauer and Bryant, 2004) and InterProScan (Mitchell et al., 2015). All *C. elegans* homologous genes inferred to encode components of the ubiquitination pathway in *H. contortus* were mapped to chromosomes in the latest version of the genome of *H. contortus* (WormBase ParaSite version WBPS15; PRJEB506) using the integrative tool kit called TBtools (Chen et al., 2020).

2.3. Analysis of transcription

The transcription profiles of genes whose proteins were inferred to be involved in the ubiquitination pathway across different developmental stages of *H. contortus* – i.e. egg (E), first-stage larva (L1), second-stage larva (L2), third-stage larva (L3), fourth-stage larva (L4; male or female), and adult (male or female) – were established. Transcriptomic data for these developmental stages/-sexes of *H. contortus* were obtained from previous studies (Schwarz et al., 2013; Mohandas et al., 2015). Raw RNA-seq reads (pair-end) were processed using trim_galore (https://zenodo.org/badge/latestdoi/62039322). Following an assessment of quality using the programs FastQC (https://www.bioinformatics.babraham.ac.uk/projects/fastqc/) and MultiQC (Ewels et al., 2016), clean reads were mapped to the genome using HISAT2 (Pertea et al., 2016). SAMtools (Li et al., 2009) was used to sort the mapped file obtained from HISAT2. For individual genes, transcriptional levels in fragments per kilobase per million (FPKM) were estimated using the assembler StringTie (Pertea et al., 2016), and normalised (z-score). GFF3 files needed for StringTie assembly were obtained from WormBase ParaSite (version WBPS15; https://parasite.wormbase.org/; Howe et al., 2017). Normalised transcription levels of individual genes were displayed in a heat map using TBtools (Chen et al., 2020).

2.4. Structure modelling and sequence comparison

The program AlphaFold (v2.0) was used to predict the three-dimensional structures of proteins inferred to be within the ubiquitination pathway (Jumper et al., 2021). Proteins of >2500 residues in length were excluded due to the technical limitations (relating to CPU, GPU and/or RAM). The program TM-align (Zhang and Skolnick, 2005) was used to structurally align homologous sequences of *H. contortus*, *C. elegans* and *O. aries* (in a pairwise manner). Structural similarity was expressed as a template modelling (TM) score, with a score of >0.5 indicating that two structures are similar and related, and a score of <0.2 indicating that they are unrelated. Structures were compared and displayed using the program UCSF ChimeraX (Pettersen et al., 2021). The program Clustal W (Larkin et al., 2007) was used for the alignment of protein sequences.

3. Results

3.1. Constructing the ubiquitination pathway model for H. contortus

We identified 215 *H. contortus* homologues of genes encoding proteins involved in the ubiquitination pathway of *C. elegans* (Supplementary Table S2), including Ub (n = 3 genes), E1 (n = 1 gene), E2 (21), HECT domain E3 (eight), U-box domain E3 (four), RING finger domain E3 (71), cullin-based complex E3 (63), APC/C complex E3 (11) and DUB (33). All inferred protein-coding genes were mapped to ubiquitination pathway components of *C. elegans* to construct a model for *H. contortus* (Figs. 1 and 2).

3.2. Genes and protein features

We inferred basic features of the respective genes (n = 215) and encoded proteins for *H. contortus*, including coding sequence (CDS) length, amino acid sequence length, theoretical pI, MW and protein domain architecture (Supplementary Table S2; Supplementary Fig. S1). The theoretical pIs ranged from 4.2 (*Hc*-UBC-3) to 11.4 (*Hc*-F08G12.5), with a mean of 6.7. The molecular weight of proteins ranged from 8.6 kDa (*Hc*-NED-8) to 426.9 kDa (*Hc*-EEL-1), with a median of 50.9 kDa. Domain architecture analysis revealed the positions of key functional domain(s). For instance, *Hc*-UBQ-1-A and -B contain eight and six UBQ domains, respectively, whereas *Hc*-UBQ-2 only has one such domain (Fig. 3). In *O. aries*, 145 orthologues of genes encoding proteins in the ubiquitination pathway of *H. contortus* were identified (Supplementary Table S3).

3.3. Chromosomal localisation

The genes encoding proteins of the ubiquitination pathway model of *H. contortus* are located on six chromosomes (Supplementary Fig. S2). Most genes (n = 57) are on chr3; 48, 40, 30 and 28 genes are on ch1, ch2, ch4 and ch5, and only 12 genes are on chX. Of the 251 genes, 35 genes clustered within five regions (I–V) on three chromosomes (Supplementary Fig. S2). These five regions each encode ubiquitin conjugating and RING domain ubiquitin ligases; regions I, II and III encode DUB, regions IV and V encode Ub, and regions I, III and V encode APC/C ubiquitin ligase subunits.

3.4. Transcription in different developmental stages of H. contortus

We investigated the transcription profiles of genes whose proteins are involved in the ubiquitination pathway in different developmental stages of *H. contortus*. Three genes encoding Ub – i.e. *Hc-ubq-1-a*, *Hc-ubq-1-b* and *Hc-ubq-2* – had the highest transcription levels in all stages, compared with all other genes (Supplementary Table S4). Ubiquitin-coding genes had high transcription in the egg (*Hc-ubq-1-a* and *Hc-ubq-1-b*) and L1 (*Hc-ubq-2*). The E1-coding gene (*Hc-uba-1*) had a high transcription level in the egg stage, and the 21 E2-coding genes were differentially transcribed among distinct developmental stages. The HECT domain- and U-box domain-ubiquitin ligase (E3)-coding genes, *Hc-hecw-1*, *Hc-Y92H12A.2*, and *Hc-udf-2*, had relatively high transcription levels in the L3 stage. The transcription levels of *Hc-chn-1*, *Hc-wwp-1* and *Hc-oxi-1* were highest in adult females, whereas *Hc-prp-19*, *Hc-etc-1* and *Hc-cyn-4* were highest in eggs (Fig. 4).

We clustered genes coding for RING finger domain proteins according to their FPKM values to identify genes with similar transcription profiles (Supplementary Fig. S3). RING finger domain-coding genes had relatively high transcription levels in the egg

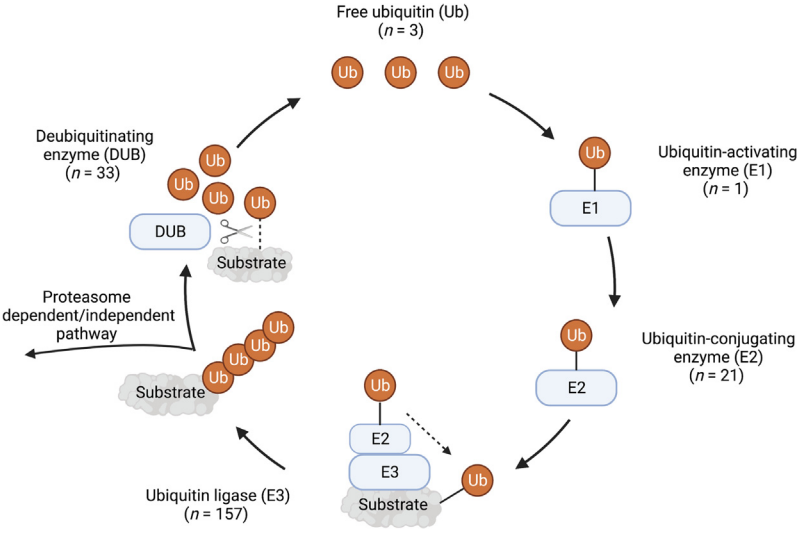

Fig. 1. Ubiquitination pathway model proposed for *Haemonchus contortus*. Pathway components are indicated, including ubiquitin (Ub), ubiquitin-activating enzyme (E1), ubiquitin-conjugating enzyme (E2), ubiquitin ligase (E3) and deubiquitinating enzyme (DUB). Ub is activated by E1; E1 transfers Ub to E2; E2 binds E3 and transfers Ub to a substrate. Polyubiquitination of a substrate results from rounds of conjugation, and plays a key role in various cellular processes via a proteasome-dependent or -independent process/pathway. DUB can cleave ubiquitin from the substrate, and Ubs are recycled. Numbers of genes encoding protein components involved in the pathway are indicated in parentheses.

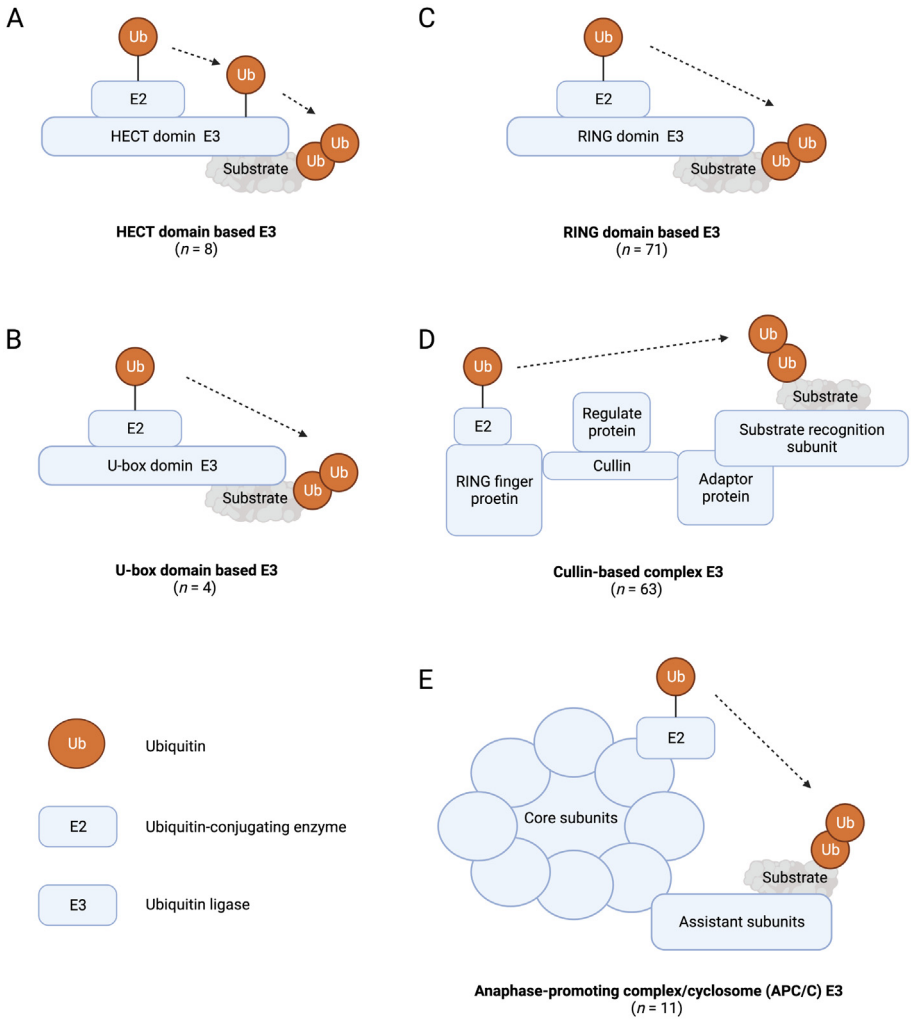

Fig. 2. Different types of ubiquitin ligase (E3) proposed for *Haemonchus contortus*. Five major classes of E3s are inferred for *H. contortus* (see A–E). (A) HECT domain E3s – the HECT domain is involved in binding the E2; ubiquitin (Ub) is transferred from E2 to E3, and then E3 transfers Ub to the substrate. (B) U-box domain E3s – the U-box domain is involved in binding the E2. The Ub is transferred to the substrate from E2. (C) Monomeric RING finger E3 – the RING finger domain is involved in binding the E2; Ub is transferred from E2 to the substrate. (D and E) Multi-subunit complexes which contains a RING finger protein – in complexes, the RING finger protein binds E2, and the substrate recognition subunits (SRS) bind the substrate; the multi-subunit can be subdivided into two subclasses (i.e. D and E). (D) Cullin-based complexes – cullin builds a scaffold that binds the RING finger protein on the C-terminus and the adaptor protein on the N-terminus. The adaptor protein binds SRS via specific domains. Regulatory proteins are covalently attached to cullin to modulate the activities of the complex. (E) Anaphase promoting complex/cyclosome (APC/C). The APC contains nine core proteins and two assistant subunits. The *n* in parentheses represents the number of genes identified in *H. contortus*.

stage (*Hc*-C06A5.8, *Hc*-T02C1.2, *Hc-rbx-2*, *Hc*-ZC13.1, *Hc*-C56A3.4 and *Hc-prx-2*), in male L4 and adult stages (*Hc*-C15F1.5, *Hc-mib-1*, *Hc-marc-1* and *Hc-tag-314*) and in female (L4 and adult) stages (*Hc*-Y38F1A.2, *Hc*-F08G12.5, *Hc-par-2*, *Hc*-B0281.3, *Hc-zhp-3*, *Hc*-B0383.6 and *Hc*-C34F11.1).

The results of cluster analysis (Supplementary Fig. S4) show that particular gene groups encoding cullin-based complex components were co-transcribed at high levels in the egg (*Hc-elb-1*, *Hc-bath-38*, *Hc-spop-1*, *Hc-tag-30*, *Hc*-T05B11.1 and *Hc-bath-41*), the L2 and L3 stages (*Hc-elc-1*, *Hc*-T07E3.4, *Hc*-B0564.9, *Hc-fbxl-1*, *Hc*-F40H3.1 and *Hc*-F10B5.3), male L4 and adult (*Hc*-Y6E2A.10, *Hc*-ZK418.2, *Hc-kel-10*, *Hc*-ZK973.8, *Hc*-C18E9.8 and *Hc*-C25G4.8) and female L4 and adult worms (*Hc-cyk-7*, *Hc-skpt-1*, *Hc-ned-8* and *Hc*-F47B10.9) The transcription levels of individual genes coding for components of anaphase-promoting complex/cyclosome (APC/C) ubiquitin ligase (E3) (Supplementary Fig. S5) reveal that most APC/C genes were highly transcribed in the egg and lowly transcribed in the L1, L2 and L4 (male) stages of *H. contortus*.

Most DUB-coding genes that exhibited a high transcription level in the egg stage had low transcription levels in L1, L2 and L4 (male) stages, except *Hc*-F37A4.5 and *Hc-ubh-1*, which were both highly transcribed in male L4 and lowly transcribed in the egg (Supplementary Fig. S6).

3.5. Protein structure prediction and comparison

We predicted the three-dimensional structures of proteins linked to the ubiquitination pathways of *H. contortus*, *C. elegans* and *O. aries* (https://github.com/vetscience/Zheng_Y_1). Pairwise comparisons with *C. elegans* and *O. aries* revealed 162 and 107 *H. contortus* proteins that had TM scores of >0.5 (Supplementary Fig. S7A), with scores being higher for comparisons with *C. elegans*, and the top 10% of proteins having scores of >0.9 Supplementary (Fig. S7A). TM scores were highest for proteins in the Ub, E1 and E2 groups, with the top 25% of proteins having scores of >0.9, and >75% of proteins having scores of >0.5. By contrast, TM scores were lower for E3s and DUB proteins, 25% and 50% of which had scores of <0.5 and <0.7, respectively (Supplementary Fig. S7B). For E1, *H. contortus Hc*-UBA-1 had 77% sequence similarity to *C. elegans* UBA-1 and 64% to its orthologue in *O. aries*

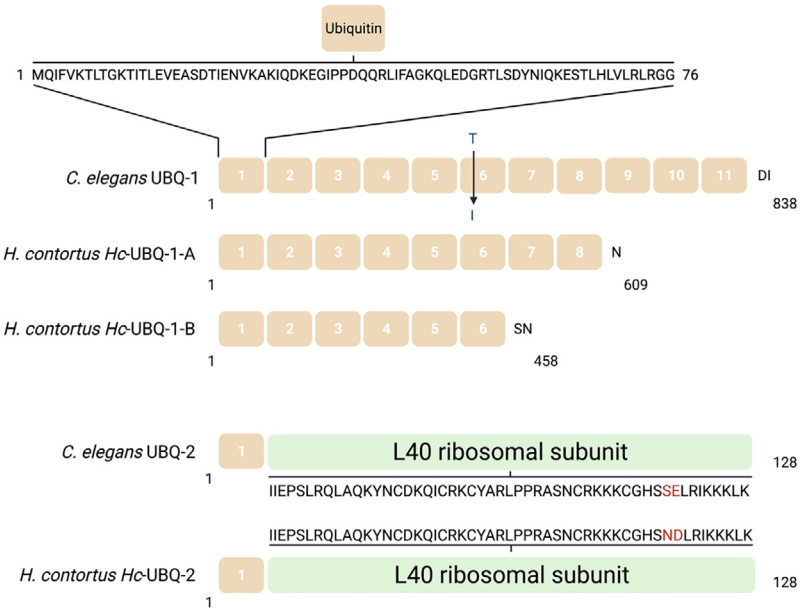

Fig. 3. Comparative analysis of protein sequences predicted from genes encoding ubiquitin (Ub) in *Caenorhabditis elegans* and in *Haemonchus contortus*. Each line (yellow box) contains 76 amino acids, and ubiquitin repeats are indicated. UBQ-1 encodes 11 tandem repeats which are identical to one another, with the exception of repeat 6; here, a leucine replaces a threonine residue at position 9 (blue). The *Hc*-UBQ-1-A and *Hc*-UBQ-1-B have eight and six tandem repeats, respectively. *Hc*-UBQ-2 and *Caenorhabditis elegans* UBQ-2 are the same in length, and each of their Ub-coding regions are identical. Only in the L40 subunit-coding region are there two distinct amino acid differences (red). Black numbers indicate the first and last amino acids in a protein sequence. Amino acids after the ubiquitin repeats are indicated (DI, N and SN).

(XP_011962196_1), with the active site being conserved (Fig. 5). TM scores of 0.93 (*H. contortus* versus *C. elegans*) and 0.94 (*H. contortus* versus *O. aries*) indicated clear structural conservation of E1 among all three species.

4. Discussion

Although the ubiquitination system is generally considered to be conserved constitutionally, structurally and functionally among eukaryotes (Michelle et al., 2009; Zuin et al., 2014), very little work has been done to substantiate this assumption, and parasitic helminths had not been considered. Given that parasitic nematodes are so unique, in terms of their biology and existence, one would expect some marked differences in the way proteins are processed and degraded within cells and tissues, and also at the parasite-host interface. The significant advances made recently in the areas of parasitic nematode genomics, transcriptomics and proteomics now provide unprecedented molecular resources and tools for comparative investigations. This is particularly the case for the barber's pole worm, *H. contortus*, which is now considered as an exceptional parasitic nematode model and whose genome is chromosome-contiguous (Doyle et al., 2020; Ma et al., 2020). Compared with the free-living nematode *C. elegans*, whose ubiquitination pathway has been extensively explored with considerable research (see Kipreos, 2005; Papaevgeniou and Chondrogianni, 2014), almost nothing is known about this pathway in *H. contortus*. Comparative studies with *C. elegans* are particularly pertinent because this free-living nematode is relatively closely related to *H. contortus* (Bürglin et al., 1998; Gilleard, 2004) and because it is arguably the best-characterised metazoan organism – in relation to most, if not all, aspects of biology, cellular and molecular biology (Harris et al., 2020). For these reasons, we constructed here a ubiquitination pathway model for *H. contortus*, with a perspective on comparing its molecular composition with *C. elegans* and, importantly, on building a foundation for future experimental work on the pathway and for identifying molecules in this pathway as potential targets for new nematocides.

The set of 215 genes and encoded proteins representing the ubiquitination pathway in *H. contortus* was compared with the set of >399 genes in *C. elegans*. Similarities were seen in the composition of ubiquitin (three genes found in *H. contortus* and two in *C. elegans*), ubiquitin-activating (both with one gene) and ubiquitin-conjugating enzymes (21 genes in *H. contortus* and 22 genes in *C. elegans*). Marked differences were seen in the E3s and DUBs, where not only less were present in *H. contortus* than that in *C. elegans*, but also E3 complexes were distinct between the two species. These differences might reflect uniqueness of the ubiquitination pathway in *H. contortus*.

Most genes involved in the ubiquitination pathway had high transcription levels in the egg stage, indicating marked ubiquitination during embryo development, body morphogenesis, DNA replication and apoptosis, similar to the situation in *C. elegans* (see Kipreos, 2005). During the transition from egg to L1, many ubiquitination pathway genes were downregulated, except for *Hc-ubq-2*, which demonstrates a low level of ubiquitination activities in this stage. In the L2 and L3 stages, most genes exhibited moderate transcription levels compared with other stages. However, some cullin-based components coding genes (*Hc-elc-1*, *Hc*-T07E3.4, *Hc*-B0564.9, *Hc-fbxl-1*, *Hc*-F40H3.1 and *Hc*-F10B5.3) reached peaks in the L2 and L3 stages (Supplementary Fig. S4). We predict that these genes might have protein-macromolecule activities and may regulate the defaecation rhythm, based on knowledge of homologues in *C. elegans* (see Kim et al., 2012; Hwang et al., 2015). In addition, the alteration of transcription of different ubiquitination component-coding genes might be a response to a reduced food intake by the L2 and L3 stages, as indicated in a previous study (Laing et al., 2013). In *H. contortus*, the L4 is the first blood-feeding stage, and many metabolic processes change in xL3 and L4 stages during the transition to parasitism (Harder, 2016; Schwarz et al., 2013; Wang et al., 2018). We observed marked differences in transcription of selected genes encoding ubiquitin ligase between male L4 and female L4 stages. Interestingly, the same patterns are also observed between male adult and female adult stages (Supplementary Figs. S2–S6). Pre-

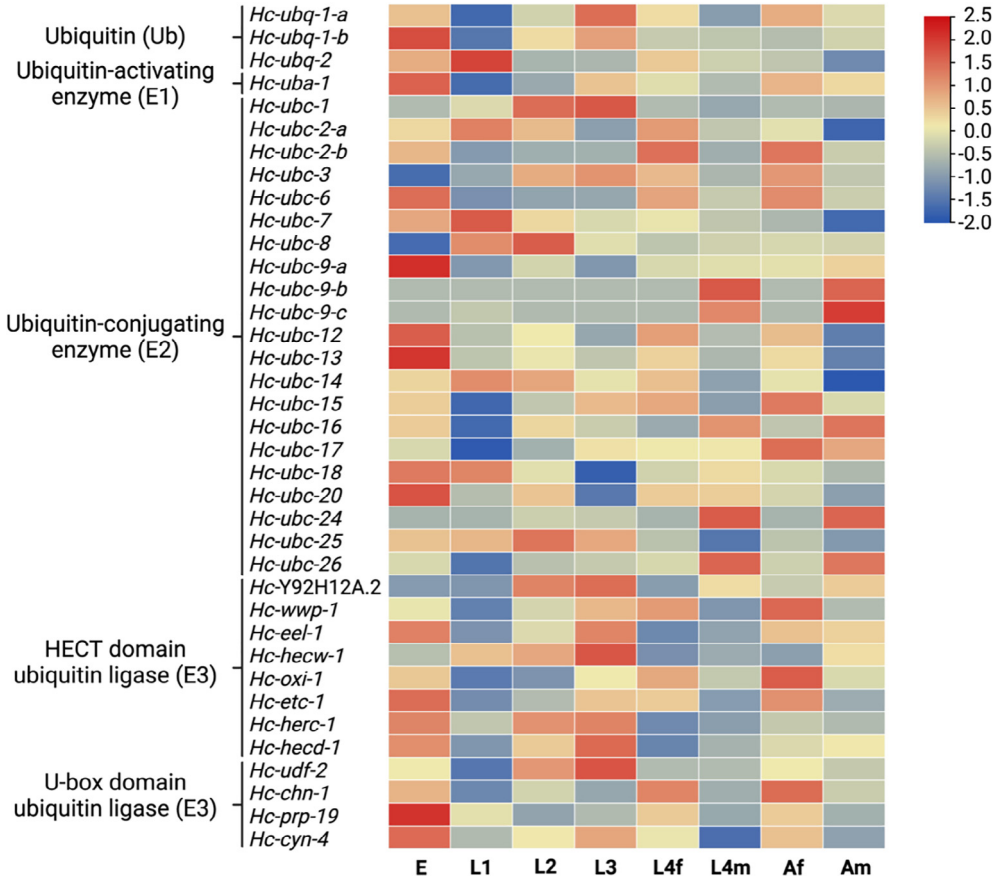

Fig. 4. Transcription profiles of selected genes in the ubiquitination pathway in different developmental stages: egg; first-, second- or third-stage larvae; female or male fourth-stage larvae; female or male adults (respective abbreviations: E; L1, L2 or L3; L4f or L4m; Af or Am) of *Haemonchus contortus*. The colour scale indicates normalised fragments per kilobase per million (FPKM) values. Genes encoding ubiquitin (Ub), ubiquitin-activating enzyme (E1), ubiquitin-conjugating enzyme (E2), HECT domain ubiquitin ligase (E3) and U-box domain ubiquitin ligase (E3).

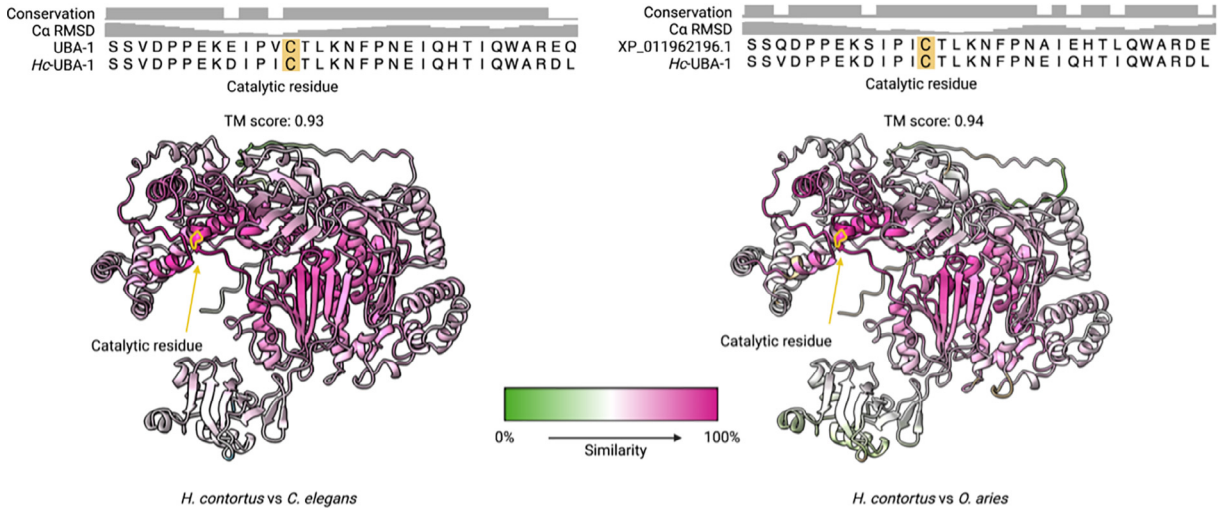

Fig. 5. Three-dimensional structural models for the ubiquitin-activating enzyme of *Haemonchus contortus* (*Hc*-UBA-1) compared with its orthologues in *Caenorhabditis elegans* E1 (UBA-1) and in *Ovis aries* E1 (NCBI database accession XP_011962196.1) in a pairwise manner. Conserved regions are in pink, and divergent ones in green. The catalytic residue in each protein sequence and structure is indicated in yellow. Template modelling (TM) scores of structural matches are indicated.

sumably, these apparently female-specific genes are associated with activities of embryogenesis, and the male-specific genes are related to sperm production. Apart from these highly transcribed genes, some genes exhibited limited transcription, particularly the E3 coding genes. A possible explanation might be that many E3s are substrate-specific enzymes, and that they do not need to be as highly transcribed as ubiquitin in cells, as in *C. elegans* (see Kipreos, 2005). The nature and levels of transcription of the different ubiquitination pathway genes in *H. contortus* likely reflect a dynamic process that governs/regulates post-translational modification and the homeostasis of proteins in different developmental stages of *H. contortus*.

The present results show that Ub, E1 and E2 in *H. contortus* are relatively conserved between *H. contortus* and *C. elegans*, with Ub being most conserved among species, in accordance with previous studies (Pickart and Eddins, 2004). Indeed, the domains in the Ubs are almost identical between the two nematodes (Fig. 3), with two forms of Ub present in both species, namely polyubiquitin (encoded by *Hc-ubq-1* and *ubq-1*), and ubiquitin plus an L40 ribosomal protein (represented by *Hc-ubq-2* and *ubq-2*) (cf. Jones and Candido, 1993). These forms are also present in other eukaryotic species, from yeast to humans, and are recognised as universal forms in eukaryotes (Özkaynak et al., 1984, 1987; Scheel, H., 2005 – Comparative analysis of the ubiquitin–proteasome system in *Homo sapiens* and *Saccharomyces cerevisiae*. PhD thesis, University of Cologne, Cologne, Germany). In addition, the transcription profiles of these genes were similar among stages of both nematodes (with respect to other genes), indicating that ubiquitin plays a conserved and indispensable role in these eukaryotes. As the specific knockdown of *ubq-1* and *ubq-2* genes in *C. elegans* causes one-cell stage arrest during the meiotic divisions (see Gönczy et al., 2000; Kipreos, 2005), *Hc-ubq-1-a*, *Hc-ubq-1-b* and *Hc-ubq-2* are more likely essential for meiosis and development of *H. contortus*.

Similar to many eukaryotes (cf. Panchamia et al., 2020), both *H. contortus* and *C. elegans* only have a single gene coding for E1, which is conserved and plays an indispensable role in various cellular functions. In accord with previous evidence (Panchamia et al., 2020), E1 was relatively conserved in primary protein sequence and structure (Fig. 5), with invariable ubiquitin-activating enzyme active sites indicating conserved biological function. Based on evidence for *C. elegans* (see Kulkarni et al., 2008), we propose that E1 (encoded by *Hc-uba*-1) is linked to embryonic development, body size and fertility.

E2 is recognised as an important ubiquitin transferring platform in the ubiquitination pathway and plays crucial roles in many cell functions such as immune responses, cell development, and DNA damage repair (van Wijk and Timmers, 2010; Liu et al., 2020). In *H. contortus*, 21 E2s including two UEVs were identified, which is similar to the 22 E2s and three UEVs in *C. elegans* (see Jones et al., 2002; Kipreos, 2005), and no evidence of gene family expansion. Of all E2s, *ubc-2* and *ubc-14* are the only UBC-coding genes essential for embryonic viability in *C. elegans* (see Jones et al., 2002; Kipreos, 2005), which indicates that *Hc-ubc-2-a*, *Hc-ubc-2-b* and *Hc-ubc-14* might be essential genes in *H. contortus* (Supplementary Table S5). Interestingly, in *C. elegans* UBC-9 and UBC-12 do not conjugate ubiquitin, but rather SUMO and NED-8 (Ub-like proteins) (see Jones and Candido, 2000; Jones et al., 2002), although they are members of the UBC gene family. Here, we speculate that *Hc*-UBC-9-A, *Hc*-UBC-9-B, *Hc*-UBC-9-C and *Hc*-UBC-12 conjugate their targets in the same manner. Most E2s of *H. contortus* are structurally similar (TM > 0.5) to their *C. elegans* orthologues (Supplementary Table S2), indicating mechanistic and functional conservation at the molecular level.

Unlike the Ub-E1-E2 elements, there were marked differences in the number and sequences of E3s in the ubiquitination pathway between *H. contortus* (n = 157) and *C. elegans* (n > 273) (cf. Supplementary Tables S1and S2), suggesting marked structural and functional divergences between these species. The five structural variants of E3s, i.e. HECT domain E3s, U-box domain E3s, monomeric RING finger E3s, cullin-based E3 complexes and anaphase-promoting complex/cyclosome complexes (APC/C) E3 (cf. Fig. 2) predicted for *H. contortus*, were all represented in *C. elegans* but in higher numbers, suggesting functional distinctions in the specific binding of individual forms of E3s to particular substrates and to E2 at the final step of ubiquitination (cf. Finley et al., 2012; Zheng and Shabek, 2017). The differences in numbers, sequences and structures of select E3s of *H. contortus* from respective host orthologues (Supplementary Tables S2 and S3) suggest that some of these proteins may be selective drug targets, but this proposal requires further and detailed testing.

Currently, the functions of select E3s identified in *H. contortus* can only be suggested based on experimental findings available for *C. elegans*. Three HECT domain E3s with significant homology to molecules in *H. contortus* have been explored in *C. elegans*. RNA interference (RNAi)-based knockdown of *eel-1*, *etc-1* and *wwp-1* are associated with low-level embryonic lethality, germline deficiency and embryonic lethality, respectively (Papaevgeniou and Chondrogianni, 2014). Of all U-box domain E3s, four homologues (designated CHN-1, CYN-4, UDF-2 and PRP-19) were identified in both *H. contortus* and *C. elegans*, all of which have been functionally studied in *C. elegans*. RNAi-based silencing of *chn-1* showed deficiency in larval development and viability (see Khan and Nukina, 2004), whereas knockdown of *cyn-4* caused masculinisation of the germline and embryonic arrest (see Graham et al., 1993), and the silencing of *udf-2* and *prp-19* caused increased protein expression/feminisation of the germline (see Shimada et al., 2006) and embryonic lethality/sterility (Hebeisen et al., 2008), respectively.

Of the many RING finger domain E3 coding genes present in both *H. contortus* and *C. elegans*, we can only suggest functions for RING finger domain E3s in *H. contortus* based on evidence for *C. elegans*. Thus, at this stage, specific silencing of *rnf-5* and *rfp-1* cause body wall disorganisation (see Broday et al., 2004) and L1-stage larval arrest (see Crowe and Candido, 2004), respectively. In the absence of functional validation in *H. contortus*, we predict, based on evidence for *C. elegans*, that some of these essential molecules might be useful anthelmintic target candidates to pursue, provided that they are sufficiently distinctive from host homologues (specific/selective).

Of the multi-subunit E3 complexes, homologues of two well-structured complexes, called SCF-type and APC/C, were found in *H. contortus* (Fig. 2). We propose an SCF topology in which cullin (*Hc*-CUL-1, *Hc*-CUL-2, *Hc*-CUL-3 and *Hc*-CUL-4) builds a scaffold that binds the RING finger protein on the C-terminus and the adaptor protein (*Hc*-SKR-1-A, *Hc*-SKR-1-B, *Hc*-ELB-1, *Hc*-ELC-1 and *Hc*-DDB-1) at the N-terminal end; the adaptor protein binds SRS through specific domains (F-box and BTB domain). Regulated proteins (*Hc*-NED-8) are covalently attached to the cullin, thereby modulating the activities of the complexes (Fig. 2D). Interestingly, the number of F-box domain and BTB domain genes identified in *H. contortus* is much less than that in *C. elegans*, suggesting that the number of different SCF complexes is lower in *H. contortus*. Compared with the SCF complex, the APC/C is conserved; for the latter, nine core subunits coding genes and two accessory subunits coding genes were identified in *H. contortus*, the same number as in *C. elegans* (Fig. 2E). Genetic experimentation is needed to explore the cellular roles of components of the multi-subunit E3 complex in *H. contortus*.

The identification of DUBs in *H. contortus* is crucial for exploring the process that removes ubiquitin from the conjugated substrates. Similar to E3s, DUBs are divergent in sequence and structure between *H. contortus* and *C. elegans*, with 33 DUBs identified in the former and 41 in the latter species (Supplementary Tables S1 and S2); DUBs are divided into five subclasses: OTU domain DUB, JAMM domain DUB, USP domain DUB, UCH domain DUB and MJD domain DUB (Nijman et al., 2005). These divergent features indicate that DUBs might be drug targets in *H. contortus*, given that they are valid targets for neurodegenerative diseases (see Lim et al., 2020) and even for Coronaviruses (e.g., SARS-CoV-2) of humans (Clemente et al., 2020). However, currently, there is limited information on the functions of individual DUBs compared with other components in the ubiquitination pathway of *C. elegans*. Nonetheless, RNAi of *CeUBP130* causes cell division defective embryos in *C. elegans* (see Lee et al., 2001), suggesting genes coding for select DUBs might be essential in *H. contortus*.

Using extensive, publicly available genomic and transcriptomic resources, we have constructed a ubiquitination pathway model for *H. contortus*, guided by information available in *C. elegans* – the best characterised metazoan organism. Comparisons of this pathway between *H. contortus* and *C. elegans* revealed the nature and extent of variation and transcription of genes encoding key elements of this pathway. Consistent with prior assumptions of conservation in eukaryotes (see Pickart and Eddins, 2004), three components (Ub, E1 and E2) were relatively conserved, in terms of the numbers of encoding genes, and in sequence and structure, whereas other elements (of E3 and DUBs) were only moderately conserved or divergent.

The former (conserved) molecules would appear to play roles that are conserved in even evolutionarily distant taxa, and the latter (variable) elements appear to be unique to *Haemonchus*, and might be responsible for maintaining a parasitic mode of existence. If these variable elements are indeed conserved among related strongylid nematodes and prove to have similar functions, then the divergence in sequence and structure of these molecules from those of their hosts might indicate the potential to be useful targets for new anthelmintics, provided that they are essential for life, are highly transcribed in most developmental stages and are unique to this nematode group. At this stage, we expect that these molecules are essential, but this proposal will require experimental validation by gene or chemical knockdown. Given that some drugs are available that target homologous elements in humans (Zhang et al., 2020) or select parasites (e.g., *Schistosoma mansoni*; see Barban do Patrocínio et al., 2021), it is possible that some commercially-available and U.S. Food and Drug Administration (FDA)-approved compounds could be modified by medicinal chemistry, and be subjected to structure–activity relationship studies conducted in *H. contortus* to achieve selective killing of all developmental stages of this parasite without affecting host (e.g., ovine) cells. In addition to providing a prospect for anthelmintic discovery, the present study also addresses fundamental aspects and provides a solid foundation for investigations of post-translational regulation, protein cycle mechanism and parasite-host relationship in *H. contortus* and related nematodes which warrant future investigations. Experiences made in the current study also show that, from a technical perspective, machine learning-driven protein structure prediction using advanced software packages, such as AlphaFold v2.0 (Jumper et al., 2021) and/or RoseTTAFold (Baek et al., 2021), can serve as powerful tools to enhance the annotation of proteomic data inferred from well-assembled genomes and/or transcriptomes of *H. contortus* and other parasitic nematodes.

Acknowledgements

This work was supported by grants from the Australian Research Council (ARC), namely LP180101085 (RBG), LP180101334 (NDY) and LP190101209 (RBG), and industry partners including Yourgene Health Singapore and PhylumTech (Argentina). The funders had no role in study design, data collection and analysis, decision to publish, or preparation of the manuscript. Ross S. Hall provided informatic support. YTZ was supported by a Melbourne Research Scholarship and the Rowden White Scholarship (Australia). Figures were created with BioRender.com. This research was undertaken using the LIEF HPC-GPGPU Facility, hosted at the University of Melbourne, Australia, established with the assistance of ARC grant LE170100200.

Appendix A. Supplementary data

Supplementary data to this article can be found online at https://doi.org/10.1016/j.ijpara.2022.06.001.

References

Archibald, A.L., Cockett, N.E., Dalrymple, B.P., Faraut, T., Kijas, J.W., Maddox, J.F., McEwan, J.C., Hutton Oddy, V., Raadsma, H.W., Wade, C., Wang, J., Wang, W., Xun, X., 2010. The sheep genome reference sequence: a work in progress. Anim. Genet. 41, 449–453.

Baek, M., DiMaio, F., Anishchenko, I., Dauparas, J., Ovchinnikov, S., Lee, G.R., Wang, J., Cong, Q., Kinch, L.N., Schaeffer, R.D., Millán, C., Park, H., Adams, C., Glassman, C.R., DeGiovanni, A., Pereira, J.H., Rodrigues, A.V., van Dijk, A.A., Ebrecht, A.C., Opperman, D.J., Sagmeister, T., Buhlheller, C., Pavkov-Keller, T., Rathinaswamy, M.K., Dalwadi, U., Yip, C.K., Burke, J.E., Garcia, K.C., Grishin, N. V., Adams, P.D., Read, R.J., Baker, D., 2021. Accurate prediction of protein structures and interactions using a three-track neural network. Science 373 (6557), 871–876.

Barban do Patrocínio, A., Cabral, F.J., de Paiva, T.H., Magalhães, L.G., Paula, L.A.d.L., Brigato, O.M., Guerra-Sá, R., Rodrigues, V., 2021. Deubiquitinating enzymes as possible drug targets for schistosomiasis. Acta Trop. 217, 105856.

Behuliak, M., Celec, P., Gardlik, R., Palffy, R., 2005. Ubiquitin–the kiss of death goes Nobel. Will you be quitting. Bratisl. Lek. Listy 106, 93–100.

Broday, L., Kolotuev, I., Didier, C., Bhoumik, A., Podbilewicz, B., Ronai, Z.E., 2004. The LIM domain protein UNC-95 is required for the assembly of muscle attachment structures and is regulated by the RING finger protein RNF-5 in *C. elegans*. J. Cell Biol. 165, 857–867.

Bürglin, T.R., Lobos, E., Blaxter, M.L., 1998. *Caenorhabditis elegans* as a model for parasitic nematodes. Int. J. Parasitol. 28 (3), 395–411.

Chen, C., Chen, H., Zhang, Y., Thomas, H.R., Frank, M.H., He, Y., Xia, R., 2020. TBtools: an integrative toolkit developed for interactive analyses of big biological data. Mol. Plant 13 (8), 1194–1202.

Clemente, V., D'arcy, P., Bazzaro, M., 2020. Deubiquitinating enzymes in coronaviruses and possible therapeutic opportunities for COVID-19. Int. J. Mol. Sci. 21, 3492.

Crowe, E., Candido, E.P.M., 2004. Characterization of *C. elegans* RING finger protein 1, a binding partner of ubiquitin-conjugating enzyme 1. Dev. Biol. 265 (2), 446–459.

Daulny, A., Tansey, W.P., 2009. Damage control: DNA repair, transcription, and the ubiquitin–proteasome system. DNA Repair 8 (4), 444–448.

Doyle, S.R., Laing, R., Bartley, D., Britton, C., Chaudhry, U., Gilleard, J.S., Holroyd, N., Mable, B.K., Maitland, K., Morrison, A.A., Tait, A., Tracey, A., Berriman, M., Devaney, E., Cotton, J.A., Sargison, N.D., 2018. A genome resequencing-based genetic map reveals the recombination landscape of an outbred parasitic nematode in the presence of polyploidy and polyandry. Genome Biol. Evol. 10, 396–409.

Doyle, S.R., Tracey, A., Laing, R., Holroyd, N., Bartley, D., Bazant, W., Beasley, H., Beech, R., Britton, C., Brooks, K., Chaudhry, U., Maitland, K., Martinelli, A., Noonan, J.D., Paulini, M., Quail, M.A., Redman, E., Rodgers, F.H., Sallé, G., Shabbir, M.Z., Sankaranarayanan, G., Wit, J., Howe, K.L., Sargison, N., Devaney, E., Berriman, M., Gilleard, J.S., Cotton, J.A., 2020. Genomic and transcriptomic variation defines the chromosome-scale assembly of *Haemonchus contortus*, a model gastrointestinal worm. Commun. Biol. 3, 656.

Eddy, S., 2009. A new generation of homology search tools based on probabilistic inference. Genome Inform. 23, 205–211.

Ewels, P., Magnusson, M., Lundin, S., Käller, M., 2016. MultiQC: summarize analysis results for multiple tools and samples in a single report. Bioinformatics 32 (19), 3047–3048.

Finley, D., Ulrich, H.D., Sommer, T., Kaiser, P., 2012. The ubiquitin–proteasome system of *Saccharomyces cerevisiae*. Genetics 192, 319–360.

Gasser, R.B., von Samson-Himmelstjerna, G., 2016. *Haemonchus contortus* and Haemonchosis – Past, Present and Future Trends. Academic Press, eBook ISBN: 9780128103968.

Gasser, R.B., Schwarz, E.M., Korhonen, P.K., Young, N.D., 2016. Understanding *Haemonchus contortus* better through genomics and transcriptomics. Adv. Parasitol. 93, 519–567.

Gasteiger, E., Gattiker, A., Hoogland, C., Ivanyi, I., Appel, R.D., Bairoch, A., 2003. ExPASy: the proteomics server for in-depth protein knowledge and analysis. Nucleic Acids Res. 31, 3784–3788.

Gilleard, J.S., 2004. The use of *Caenorhabditis elegans* in parasitic nematode research. Parasitology 128 (S1), S49–S70.

Glickman, M.H., Ciechanover, A., 2002. The ubiquitin-proteasome proteolytic pathway: destruction for the sake of construction. Physiol. Rev. 82 (2), 373–428.

Goldberg, A.L., 2003. Protein degradation and protection against misfolded or damaged proteins. Nature 426 (6968), 895–899.

Gönczy, P., Echeverri, C., Oegema, K., Coulson, A., Jones, S.J.M., Copley, R.R., Duperon, J., Oegema, J., Brehm, M., Cassin, E., Hannak, E., Kirkham, M., Pichler, S., Flohrs, K., Goessen, A., Leidel, S., Alleaume, A.-M., Martin, C., Özlü, N., Bork, P., Hyman, A.A., 2000. Functional genomic analysis of cell division in *C. elegans* using RNAi of genes on chromosome III. Nature 408 (6810), 331–336.

Graham, P.L., Schedl, T., Kimble, J., 1993. More mog genes that influence the switch from spermatogenesis to oogenesis in the hermaphrodite germ line of *Caenorhabditis elegans*. Dev. Genet. 14 (6), 471–484.

Guo, W., Shang, F., Liu, Q., Urim, L., West-Mays, J., Taylor, A., 2004. Differential regulation of components of the ubiquitin-proteasome pathway during lens cell differentiation. Invest. Ophthalmol. Vis. Sci. 45, 1194–1201.

Haas, A.L., Warms, J.V., Hershko, A., Rose, I.A., 1982. Ubiquitin-activating enzyme. Mechanism and role in protein-ubiquitin conjugation. J. Biol. Chem. 257 (5), 2543–2548.

Harder, A., 2016. The biochemistry of *Haemonchus contortus* and other parasitic nematodes. Adv. Parasitol. 93, 69–94.
Harris, T.W., Arnaboldi, V., Cain, S., Chan, J., Chen, W.J., Cho, J., Davis, P., Gao, S., Grove, C.A., Kishore, R., Lee, R.Y.N., Muller, H.M., Nakamura, C., Nuin, P., Paulini, M., Raciti, D., Rodgers, F.H., Russell, M., Schindelman, G., Auken, K.V., Wang, Q., Williams, G., Wright, A.J., Yook, K., Howe, K.L., Schedl, T., Stein, L., Sternberg, P. W., 2020. WormBase: a modern model organism information resource. Nucleic Acids Res. 48, D762–D767.
Hebeisen, M., Drysdale, J., Roy, R., 2008. Suppressors of the cdc-25.1 (gf)-associated intestinal hyperplasia reveal important maternal roles for prp-8 and a subset of splicing factors in *C. elegans*. RNA 14 (12), 2618–2633.
Hershko, A., Ciechanover, A., 1998. The ubiquitin system. Annu. Rev. Biochem. 67 (1), 425–479.
Howe, K.L., Bolt, B.J., Shafie, M., Kersey, P., Berriman, M., 2017. WormBase ParaSite – a comprehensive resource for helminth genomics. Mol. Biochem. Parasitol. 215, 2–10.
Hwang, W., Artan, M., Seo, M., Lee, D., Nam, H.G., Lee, S.J.V., 2015. Inhibition of elongin C promotes longevity and protein homeostasis via HIF-1 in *C. elegans*. Aging Cell 14, 995–1002.
Johnson, M., Zaretskaya, I., Raytselis, Y., Merezhuk, Y., McGinnis, S., Madden, T.L., 2008. NCBI BLAST: a better web interface. Nucleic Acids Res. 36, 5–9.
Jones, D., Candido, E.P., 1993. Novel ubiquitin-like ribosomal protein fusion genes from the nematodes *Caenorhabditis elegans* and *Caenorhabditis briggsae*. J. Biol. Chem. 268 (26), 19545–19551.
Jones, D., Candido, E.P.M., 2000. The NED-8 conjugating system in *Caenorhabditis elegans* is required for embryogenesis and terminal differentiation of the hypodermis. Dev. Biol. 226 (1), 152–165.
Jones, D., Crowe, E., Stevens, T.A., Candido, E.P.M., 2002. Functional and phylogenetic analysis of the ubiquitylation system in *Caenorhabditis elegans:* ubiquitin-conjugating enzymes, ubiquitin-activating enzymes, and ubiquitin-like proteins. Genome Biol. 3. research0002.
Jumper, J., Evans, R., Pritzel, A., Green, T., Figurnov, M., Ronneberger, O., Tunyasuvunakool, K., Bates, R., Žídek, A., Potapenko, A., Bridgland, A., Meyer, C., Kohl, S.A.A., Ballard, A.J., Cowie, A., Romera-Paredes, B., Nikolov, S., Jain, R., Adler, J., Back, T., Petersen, S., Reiman, D., Clancy, E., Zielinski, M., Steinegger, M., Pacholska, M., Berghammer, T., Bodenstein, S., Silver, D., Vinyals, O., Senior, A. W., Kavukcuoglu, K., Kohli, P., Hassabis, D., 2021. Highly accurate protein structure prediction with AlphaFold. Nature 596 (7873), 583–589.
Kallio, P.J., Wilson, W.J., O'Brien, S., Makino, Y., Poellinger, L., 1999. Regulation of the hypoxia-inducible transcription factor 1α by the ubiquitin-proteasome pathway. J. Biol. Chem. 274 (10), 6519–6525.
Khan, L.A., Nukina, N., 2004. Molecular and functional analysis of *Caenorhabditis elegans* CHIP, a homologue of mammalian CHIP. FEBS Lett. 565, 11–18.
Kiełbasa, S.M., Wan, R., Sato, K., Horton, P., Frith, M.C., 2011. Adaptive seeds tame genomic sequence comparison. Genome Res. 21 (3), 487–493.
Kim, S.-M., Jang, S.-H., Son, N., Han, C.-T., Min, K.-S., Lee, H., Hwang, S.-Y., 2012. A novel F-box protein with leucine-rich repeats affects defecation frequency and daumone response in *Caenorhabditis elegans*. Anim. Cells Syst. 16 (4), 280–288.
Kipreos, E.T., 2005. Ubiquitin-mediated pathways in *C. elegans*. WormBook 1, 1–24.
Komander, D., Rape, M., 2012. The ubiquitin code. Annu. Rev. Biochem. 81 (1), 203–229.
Kulkarni, M., Smith, H.E., Mullins, M., 2008. E1 ubiquitin-activating enzyme UBA-1 plays multiple roles throughout *C. elegans* development. PLoS Genet. 4 (7), e1000131.
Laing, R., Kikuchi, T., Martinelli, A., Tsai, I.J., Beech, R.N., Redman, E., Holroyd, N., Bartley, D.J., Beasley, H., Britton, C., Curran, D., Devaney, E., Gilabert, A., Hunt, M., Jackson, F., Johnston, S.L., Kryukov, I., Li, K., Morrison, A.A., Reid, A.J., Sargison, N., Saunders, G.I., Wasmuth, J.D., Wolstenholme, A., Berriman, M., Gilleard, J.S., Cotton, J.A., 2013. The genome and transcriptome of *Haemonchus contortus*, a key model parasite for drug and vaccine discovery. Genome Biol. 14 (8), R88.
Larkin, M.A., Blackshields, G., Brown, N.P., Chenna, R., McGettigan, P.A., McWilliam, H., Valentin, F., Wallace, I.M., Wilm, A., Lopez, R., Thompson, J.D., Gibson, T.J., Higgins, D.G., 2007. Clustal W and Clustal X version 2.0. Bioinformatics 23 (21), 2947–2948.
Lee, J., Jee, C., Lee, J.I., Lee, M.H., Lee, M.H., Koo, H.S., Chung, C.H., Ahnn, J., 2001. A deubiquitinating enzyme, UCH/CeUBP130, has an essential role in the formation of a functional microtubule-organizing centre (MTOC) during early cleavage in *C. elegans*. Genes Cells 6, 899–911.
Li, H., Handsaker, B., Wysoker, A., Fennell, T., Ruan, J., Homer, N., Marth, G., Abecasis, G., Durbin, R., 2009. The sequence alignment/map format and SAMtools. Bioinformatics 25 (16), 2078–2079.
Lim, K.-H., Joo, J.-Y., Baek, K.-H., 2020. The potential roles of deubiquitinating enzymes in brain diseases. Ageing Res. Rev. 61, 101088.
Liu, W., Tang, X., Qi, X., Fu, X., Ghimire, S., Ma, R., Li, S., Zhang, N., Si, H., 2020. The ubiquitin conjugating enzyme: an important ubiquitin transfer platform in ubiquitin-proteasome system. Int. J. Mol. Sci. 21, 2894.
Luza, S., Opazo, C.M., Bousman, C.A., Pantelis, C., Bush, A.I., Everall, I.P., 2020. The ubiquitin proteasome system and schizophrenia. Lancet Psychiatry 7 (6), 528–537.
Ma, G., Gasser, R.B., Wang, T., Korhonen, P.K., Young, N.D., 2020. Toward integrative 'omics of the barber's pole worm and related parasitic nematodes. Infect. Genet. Evol. 85, 104500.
Ma, G., Wang, T., Korhonen, P.K., Ang, C.-S., Williamson, N.A., Young, N.D., Stroehlein, A.J., Hall, R.S., Koehler, A.V., Hofmann, A., Gasser, R.B., 2018. Molecular alterations during larval development of *Haemonchus contortus* in vitro are under tight post-transcriptional control. Int. J. Parasitol. 48 (9-10), 763–772.
Ma, G., Wang, T., Korhonen, P.K., Stroehlein, A.J., Young, N.D., Gasser, R.B., 2019. Dauer signalling pathway model for *Haemonchus contortus*. Parasit. Vectors 12, 187.
Marchler-Bauer, A., Bryant, S.H., 2004. CD-search: protein domain annotations on the fly. Nucleic Acids Res. 32 (Web Server), W327–W331.
Michelle, C., Vourc'h, P., Mignon, L., Andres, C.R., 2009. What was the set of ubiquitin and ubiquitin-like conjugating enzymes in the eukaryote common ancestor. J. Mol. Evol. 68 (6), 616–628.
Mitchell, A., Chang, H.-Y., Daugherty, L., Fraser, M., Hunter, S., Lopez, R., McAnulla, C., McMenamin, C., Nuka, G., Pesseat, S., Sangrador-Vegas, A., Scheremetjew, M., Rato, C., Yong, S.Y., Bateman, A., Punta, M., Attwood, T.K., Sigrist, C.J.A., Redaschi, N., Rivoire, C., Xenarios, I., Kahn, D., Guyot, D., Bork, P., Letunic, I., Gough, J., Oates, M., Haft, D., Huang, H., Natale, D.A., Wu, C.H., Orengo, C., Sillitoe, I., Mi, H., Thomas, P.D., Finn, R.D., 2015. The InterPro protein families database: the classification resource after 15 years. Nucleic Acids Res. 43, D213–D221.
Mohandas, N., Young, N.D., Jabbar, A., Korhonen, P.K., Koehler, A.V., Amani, P., Hall, R.S., Sternberg, P.W., Jex, A.R., Hofmann, A., Gasser, R.B., 2015. The barber's pole worm CAP protein superfamily—a basis for fundamental discovery and biotechnology advances. Biotechnol. Adv. 33 (8), 1744–1754.
Nguyen, L.K., Dobrzynski, M., Fey, D., Kholodenko, B.N., 2014. Polyubiquitin chain assembly and organization determine the dynamics of protein activation and degradation. Front. Physiol. 5, 4.
Nigon, V.M., Félix, M.-A., 2017. History of research on *C. elegans* and other free-living nematodes as model organisms. WormBook 2017, 1–84.
Nijman, S.M.B., Luna-Vargas, M.P.A., Velds, A., Brummelkamp, T.R., Dirac, A.M.G., Sixma, T.K., Bernards, R., 2005. A genomic and functional inventory of deubiquitinating enzymes. Cell 123 (5), 773–786.
Ozkaynak, E., Finley, D., Solomon, M.J., Varshavsky, A., 1987. The yeast ubiquitin genes: a family of natural gene fusions. EMBO J. 6 (5), 1429–1439.
Özkaynak, E., Finley, D., Varshavsky, A., 1984. The yeast ubiquitin gene: head-to-tail repeats encoding a polyubiquitin precursor protein. Nature 312 (5995), 663–666.
Panchamia, B., Raimalani, V., Prashar, V., Kumar, M., Ratna Prabha, C., 2020. Structural and functional characterisation of the domains of ubiquitin-activating enzyme (E1) of *Saccharomyces cerevisiae*. Cell Biochem. Biophys. 78 (3), 309–319.
Papaevgeniou, N., Chondrogianni, N., 2014. The ubiquitin proteasome system in *Caenorhabditis elegans* and its regulation. Redox Biol. 2, 333–347.
Pertea, M., Kim, D., Pertea, G.M., Leek, J.T., Salzberg, S.L., 2016. Transcript-level expression analysis of RNA-seq experiments with HISAT, StringTie and Ballgown. Nat. Protoc. 11 (9), 1650–1667.
Pettersen, E.F., Goddard, T.D., Huang, C.C., Meng, E.C., Couch, G.S., Croll, T.I., Morris, J. H., Ferrin, T.E., 2021. UCSF ChimeraX: structure visualization for researchers, educators, and developers. Protein Sci. 30, 70–82.
Pickart, C.M., Eddins, M.J., 2004. Ubiquitin: structures, functions, mechanisms. Biochim. Biophys. Acta 1695 (1-3), 55–72.
Reyes-Turcu, F.E., Ventii, K.H., Wilkinson, K.D., 2009. Regulation and cellular roles of ubiquitin-specific deubiquitinating enzymes. Annu. Rev. Biochem. 78 (1), 363–397.
Schwarz, E.M., Korhonen, P.K., Campbell, B.E., Young, N.D., Jex, A.R., Jabbar, A., Hall, R.S., Mondal, A., Howe, A.C., Pell, J., Hofmann, A., Boag, P.R., Zhu, X.-Q., Gregory, T., Loukas, A., Williams, B.A., Antoshechkin, I., Brown, C., Sternberg, P.W., Gasser, R.B., 2013. The genome and developmental transcriptome of the strongylid nematode *Haemonchus contortus*. Genome Biol. 14 (8), R89.
Shimada, M., Kanematsu, K., Tanaka, K., Yokosawa, H., Kawahara, H., Sommer, T., 2006. Proteasomal ubiquitin receptor RPN-10 controls sex determination in *Caenorhabditis elegans*. Mol. Biol. Cell. 17 (12), 5356–5371.
Stroehlein, A.J., Young, N.D., Gasser, R.B., 2018. Improved strategy for the curation and classification of kinases, with broad applicability to other eukaryotic protein groups. Sci. Rep. 8, 6808.
VanDemark, A.P., Hill, C.P., 2002. Structural basis of ubiquitylation. Curr. Opin. Struct. Biol. 12, 822–830.
Wang, J., Maldonado, M.A., 2006. The ubiquitin-proteasome system and its role in inflammatory and autoimmune diseases. Cell Mol. Immunol. 3, 255–261.
Wang, T., Ma, G., Ang, C.-S., Korhonen, P.K., Koehler, A.V., Young, N.D., Nie, S., Williamson, N.A., Gasser, R.B., 2019a. High throughput LC-MS/MS-based proteomic analysis of excretory-secretory products from short-term in vitro culture of *Haemonchus contortus*. J. Proteomics 204, 103375.
Wang, T., Ma, G., Ang, C.-S., Korhonen, P.K., Stroehlein, A.J., Young, N.D., Hofmann, A., Chang, B.C.H., Williamson, N.A., Gasser, R.B., 2020a. The developmental phosphoproteome of *Haemonchus contortus*. J. Proteomics 213, 103615.
Wang, T., Ma, G., Ang, C.-S., Korhonen, P.K., Xu, R., Nie, S., Koehler, A.V., Simpson, R.J., Greening, D.W., Reid, G.E., Williamson, N.A., Gasser, R.B., 2019b. Somatic proteome of *Haemonchus contortus*. Int. J. Parasitol. 49 (3-4), 311–320.
Wang, T., Ma, G., Nie, S., Williamson, N.A., Reid, G.E., Gasser, R.B., 2020b. Lipid composition and abundance in the reproductive and alimentary tracts of female *Haemonchus contortus*. Parasit. Vectors 13, 338.
Wang, T., Nie, S., Ma, G., Korhonen, P.K., Koehler, A.V., Ang, C.-S., Reid, G.E., Williamson, N.A., Gasser, R.B., 2018. The developmental lipidome of *Haemonchus contortus*. Int. J. Parasitol. 48 (12), 887–895.
Wijk, S.J.L., Timmers, H.T.M., 2010. The family of ubiquitin-conjugating enzymes (E2s): deciding between life and death of proteins. FASEB J. 24 (4), 981–993.

Zhang, X., Linder, S., Bazzaro, M., 2020. Drug development targeting the ubiquitin–proteasome system (UPS) for the treatment of human cancers. Cancers 12, 902.
Zhang, Y., Skolnick, J., 2005. TM-align: a protein structure alignment algorithm based on the TM-score. Nucleic Acids Res. 33, 2302–2309.
Zheng, N., Shabek, N., 2017. Ubiquitin ligases: structure, function, and regulation. Annu. Rev. Biochem. 86 (1), 129–157.
Zuin, A., Isasa, M., Crosas, B., 2014. Ubiquitin signaling: extreme conservation as a source of diversity. Cells 3, 690–701.